Frequency Division Multiplexed Microwave and Baseband Digital Optical Fiber Link for Phased Array Antennas

PETER J. HEIM, MEMBER, IEEE, AND C. PHILLIP McCLAY, MEMBER, IEEE

Abstract—A frequency division multiplexed optical fiber link is described in which microwave (1 to 8 GHz) and baseband digital (1 to 10 Mb/s) signals are combined electrically and transmitted through a direct modulation microwave optical link. The microwave signal does not affect bit error rate (BER) performance of the Manchester-coded baseband digital data link. The baseband digital signal affects microwave signal quality by generating second-order intermodulation noise. The intermodulation noise power density is found to be proportional to both the microwave input power and the digital input power, enabling the system to be modeled as a mixer (AM modulator). The conversion loss for the digital signal is approximately 68 dB for a 1 GHz microwave signal and is highly dependent on the microwave frequency, reaching a minimum value of 41 dB at 4.5 GHz, corresponding to the laser diode relaxation oscillation frequency. We show that Manchester coding on the digital link places the intermodulation noise peak away from the microwave signal, preventing degradation of close carrier phase noise (< 1 kHz offset). A direct trade-off between intermodulation noise and digital link margin is developed to project system performance.

I. INTRODUCTION

HIGH-SPEED analog fiber-optic links are increasingly considered for distribution of RF signals in phased array antennas [1]–[4] because of the small size, light weight, immunity to EMI/EMP, low crosstalk, and large signal bandwidth inherent in fiber optics. Although frequency response, dynamic range, and linearity can be limiting factors [5], [6], the commercial availability of microwave modulated fiber-optic links with a 12 GHz direct modulation bandwidth, potentially extending above 20 GHz [4], [7], and of compact planar optical divider/combiner technology offers a promising alternative to conventional coaxial/waveguide RF distribution networks for many applications.

Current phased array architectures exploit GaAs MMIC technology to lower cost, reduce size, and enhance reliability by incorporating all active array components on monolithic circuits, each circuit requiring digital input signals to control phase and gain states. Distribution of these digital control signals is not as demanding as RF distribution, but providing adequate shielding to prevent crosstalk significantly increases the complexity and cost of the overall distribution network. This complexity can be reduced by taking advantage of the optical fiber's wide bandwidth to multiplex RF and digital control signals for each element or subarray on a single optical fiber.

Several options are available for transmitting RF and digital signals over a direct detection optical link, including electrical domain frequency division multiplexing (FDM), wavelength division multiplexing (WDM), and subcarrier multiplexing (SCM) [1], [8], [9]. In this paper we describe the performance of an FDM approach in which an RF/microwave signal and a baseband digital signal are combined electrically and transmitted through a conventional microwave optical link.

The primary advantage of this approach is simplicity; no additional optical or microwave components are required to combine, isolate, and detect RF and digital signals, as in WDM and SCM techniques. The primary disadvantage is that the baseband digital signal generates intermodulation noise which degrades microwave signal quality. Although intermodulation noise has been shown to be negligible when multiplexing multichannel FM video and baseband digital data [10]–[12], microwave signal quality requirements in typical phased array antenna applications (e.g. radar, SATCOM) are often more demanding than for video transmission. This paper, therefore, focuses on characterizing the intermodulation noise to allow performance projections for specific phased array applications.

II. SYSTEM DESCRIPTION

The system demonstrated in this paper simultaneously transmits a single CW RF signal (1–8 GHz) and Manchester-coded baseband digital signal (1–10 Mb/s). The system shown in Fig. 1 consists of three main components: a microwave optical link, input/output microwave bias tee networks, and a digital transmitter/receiver.

A. Microwave Optical Link

The microwave optical link consists of an InGaAsP laser diode operating at a nominal emission wavelength of 1300 nm, and an InGaAsP p-i-n photodiode receiver. An optical attenuator inserted between the laser and photodiode simulates link loss. The laser diode is broad-band impedance matched to 50 Ω by means of a series matching resistor;

Manuscript received August 29, 1989; revised November 27, 1989.
The authors are with the MITRE Corporation, Burlington Road, Bedford, MA 01730.
IEEE Log Number 8934048.

0018-9480/90/0500-0494$01.00 ©1990 IEEE

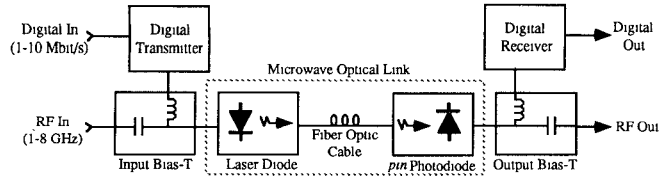

Fig. 1. Block diagram of the FDM RF/baseband digital optical fiber link.

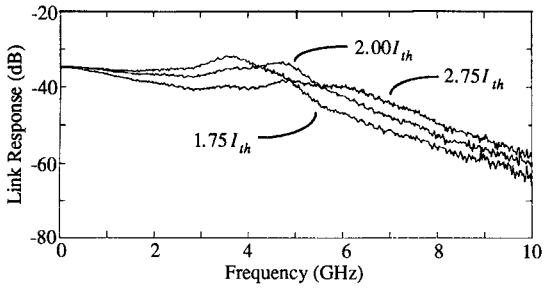

Fig. 2. Frequency response ($|S_{21}|^2$) of the microwave optical link, shown for three levels of laser diode bias current (I_{th}=14.4 mA at room temperature).

the photodiode is not matched. With the laser biased at $2I_{th}$ (threshold current I_{th}=14.4 mA at room temperature), the microwave optical link has a direct modulation bandwidth of approximately 5 GHz, as shown in Fig. 2.

B. Microwave Bias Tee

This system exploits the inherent low-pass/high-pass response of the bias tee dc/RF ports to superimpose the baseband digital signal on the dc bias network, isolating digital and RF sources at the input and filtering digital and RF channels at the output. The frequency response of the dc port limits the digital signal bandwidth. For the bias tees used in this system, the dc port has a 3 dB bandwidth of 10 MHz, allowing a maximum Manchester-coded data rate of 10 Mb/s. Custom bias networks or broad-band hybrid couplers could be used to support higher data rates.

C. Digital Transmitter/Receiver

The digital transmitter consists of a Manchester data encoder and a laser diode driver. The laser diode driver produces an adjustable current variation, ΔI, about an independently adjustable laser bias current, I_B, in response to the input digital waveform.

We chose a biphase Manchester code for the baseband digital data transmission because it offers a power spectrum with insignificant dc and low-frequency components, allowing the receiver to be ac coupled. The digital receiver must be ac coupled because simultaneous analog modulation of the laser diode results in a quiescent average optical power at the photodetector which must be rejected. A typical Manchester data spectrum generated by the digital data transmitter driving a 50 Ω load is shown in Fig. 3 for a 1 Mb/s pseudorandom data pattern ($2^{20}-1$ word length).

The baseband digital receiver is a high-impedance design with clock recovery and a Manchester data decoder.

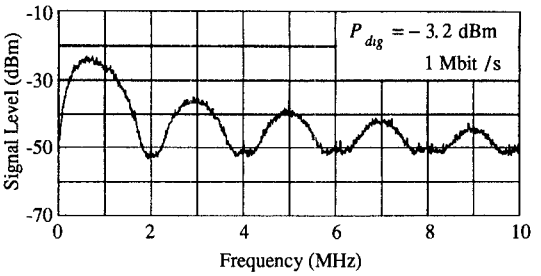

Fig. 3. Typical baseband digital data spectrum for a Manchester-coded pseudorandom data pattern ($2^{20}-1$ word length). The spectrum shown is taken at the output of the digital data transmitter driving a 50 Ω load.

The receiver operates at data rates from 1 to 5 Mb/s, with a sensitivity of −19 dBm (average received optical power) for a bit error rate of less than 10^{-9} at a 2.5 Mb/s data rate.

III. Experimental Results

Any nonlinearities in the microwave fiber-optic link introduce intermodulation distortion in the RF and baseband digital output signals, possibly degrading the analog signal-to-noise ratio (S/N) and reducing the digital link power budget. The following subsections quantify the impact of intermodulation distortion in both RF and digital channels.

A. Intermodulation Noise

Intermodulation noise generated in the RF channel by the baseband digital signal is illustrated in Fig. 4 for a 2 GHz RF input signal (+3 dBm). With no digital modulation, the microwave optical link has an output S/N of approximately 120 dBc/Hz (Fig. 4(a)). Applying digital modulation generates the sidebands observed in parts (b) and (c) of Fig. 4 for data rates of 1 Mb/s and 5 Mb/s respectively. These sidebands are second-order intermodulation products of the form

$$A\cos\left(2\pi f_{RF} \pm 2\pi f_{dig}\right)t \qquad (1)$$

where f_{RF} corresponds to the microwave signal and, for simplicity, the digital modulation spectrum is represented as a single tone at frequency f_{dig}. In most applications, the modulating frequencies are close enough that second-order intermodulation products fall out of band, while third-order intermodulation products are more troublesome. Because the RF and digital frequencies are so widely separated in this system, second-order intermodulation products are the significant in-band intermodulation components.

We determined that the laser diode is the dominant nonlinear element causing the intermodulation noise. No significant change in the intermodulation noise relative to the RF signal power was observed by varying optical input power to the photodetector over a 20 dB range, using an optical attenuator, indicating that the photodetector was not contributing to the intermodulation distortion.

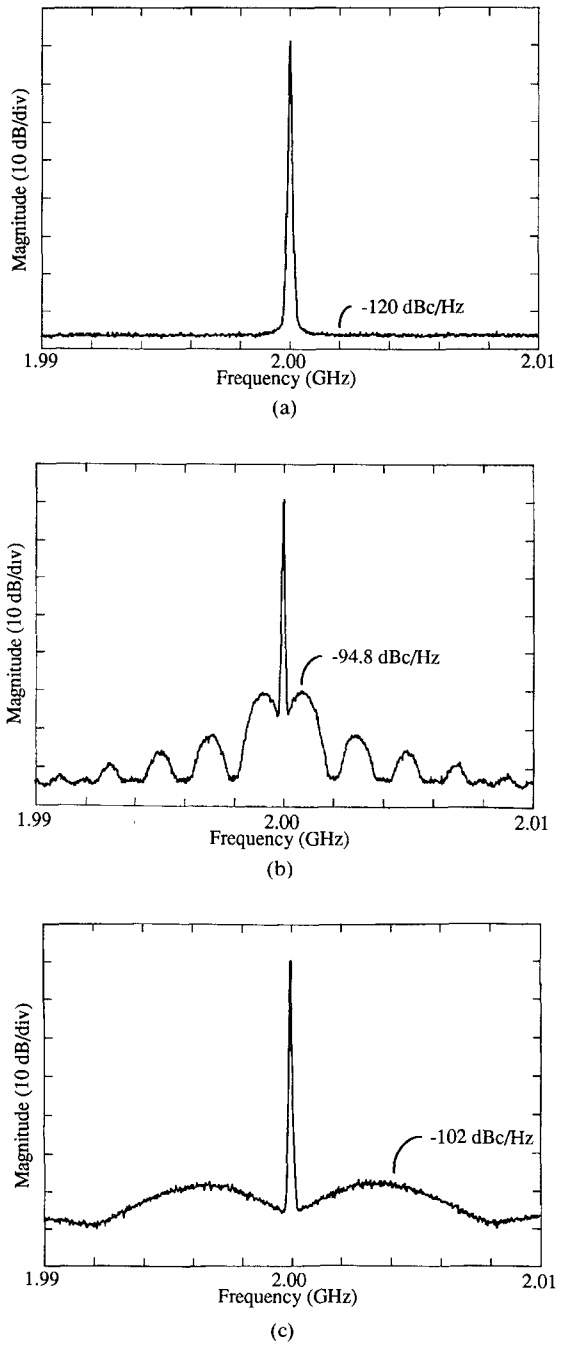

Fig. 4. (a) Microwave signal spectrum after transmission through the fiber-optic link. The spectrum analyzer IF bandwidth equals 30 kHz, yielding a signal-to-noise ratio of approximately 120 dBc/Hz. (b) Microwave signal with intermodulation noise resulting from digital data transmission at 1 Mb/s ($P_{dig} = -11$ dBm). (c) Intermodulation noise spectrum for a 5 Mb/s data transmission rate ($P_{dig} = -11$ dBm).

1) Dependence on Digital Data Rate: Increasing the digital data rate reduces the intermodulation noise power P_{im}, defined as the maximum power in a single intermodulation sideband relative to the RF carrier output power, normalized to a 1 Hz bandwidth. In the example shown in Fig. 4, we see that increasing the data rate from 1 to 5 Mb/s reduces P_{im} from -95 dBc/Hz to -102 dBc/Hz. Manchester coding ensures the peak intermodulation sideband is offset in frequency from the microwave carrier by an

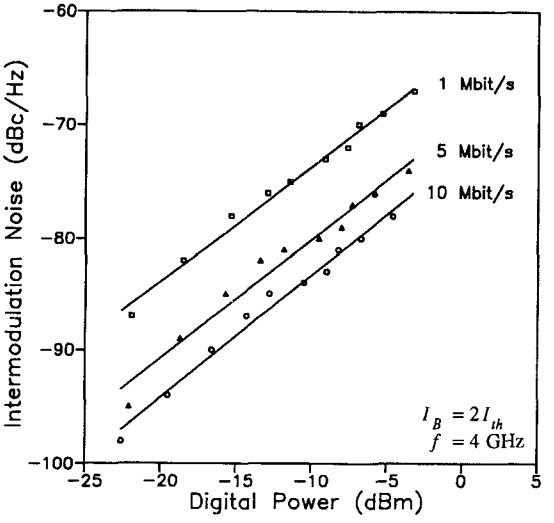

Fig. 5 Intermodulation noise power as a function of the total digital modulation power for three digital data rates where P_{RF} is fixed at +0 dBm.

amount approximately equal to the data rate. For the 1 Mb/s and 5 Mb/s data rates shown in Fig. 4, the intermodulation noise peak is offset by 750 kHz and 4 MHz, respectively. By increasing the data rate, the intermodulation noise peak can be moved arbitrarily further away from the carrier to allow filtering or placement of the intermodulation noise out of band.

2) Dependence on RF and Digital Modulation Power: To further characterize the second-order intermodulation noise, we measured P_{im} as a function of both digital modulation power P_{dig} and RF input power P_{RF}. P_{dig} is defined as the average electrical power delivered to a 50 Ω load by the digital transmitter in response to a random data pattern. This definition does not include any dc power contribution due to the bias current I_B; therefore P_{dig} depends only on the digital modulation current ΔI. We determined that for a fixed P_{RF}, the intermodulation noise power is linearly proportional to P_{dig}, as illustrated in Fig. 5. Also, for a fixed P_{dig}, the intermodulation noise power (recall that P_{im} is expressed in units relative to P_{RF}) is essentially independent of P_{RF}, as shown in Fig. 6 for P_{RF} ranging from -20 dBm to $+5$ dBm (i.e., an optical modulation index ranging from 4% to 70%). Therefore, for a given laser bias current and RF frequency, P_{dig} determines P_{im}.

The dependence of the intermodulation sidebands on P_{RF} and P_{dig} can be modeled as amplitude modulation (AM) of the RF carrier by the baseband digital signal. The power in an AM single sideband ($P_{AM,ssb}$) is given by [13]

$$P_{AM,ssb} = \frac{1}{2} k^2 P_C P_A \tag{2}$$

where P_C and P_A are the carrier and modulation powers and k is the sensitivity of the AM modulator. Letting $P_C = P_{RF}$, $P_A = P_{dig}$, and normalizing to the output RF

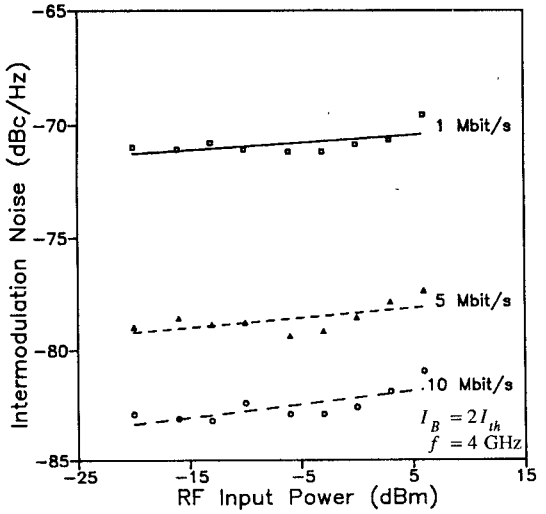

Fig. 6. Intermodulation noise power as a function of the RF input power for three digital data rates where P_{dig} is fixed at approximately −3 dBm.

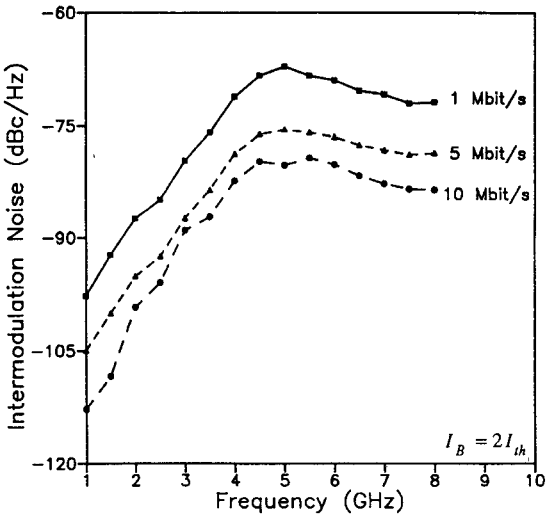

Fig 7 Intermodulation noise power as a function of the RF signal frequency for three digital data rates. P_{dig} is approximately −3 dBm for the three curves. The intermodulation noise peaks at approximately 5 GHz, which corresponds to the laser diode relaxation oscillation frequency.

power yields

$$P_{im} = \frac{1}{2} k'^2 P_{dig} \tag{3}$$

where k' differs from k by a constant due to the normalization. Note that this predicts the linear dependence on P_{dig} and an insensitivity to P_{RF} as observed in Figs. 5 and 6.

3) Dependence on Laser Bias and RF Frequency: For this system k' is not a constant but varies with I_B and RF frequency. The frequency dependence of the intermodulation noise is shown in Fig. 7. These data show that the intermodulation noise increases with RF modulation frequency at a rate of approximately 8 dB/GHz, reaching a maximum at 5 GHz, which corresponds to the laser diode relaxation oscillation frequency (see Fig. 2). This behavior

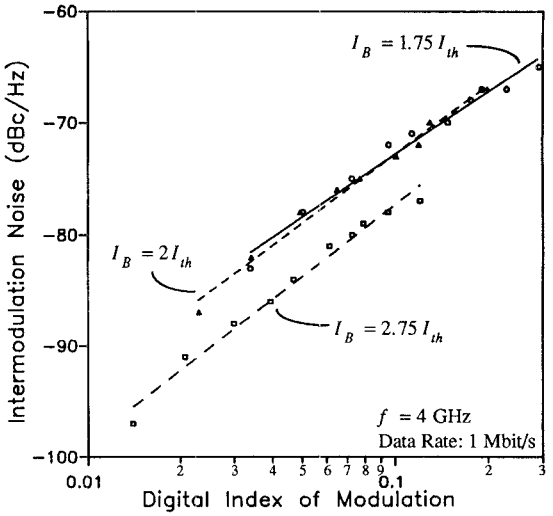

Fig. 8. Intermodulation noise power as a function of the digital index of modulation for three different laser diode bias currents.

agrees with the well-known observation that linearity degrades as operating frequency increases [14], [15], but differs from the frequency dependence of third-order intermodulation products which exhibit maxima at half the relaxation oscillation frequency [16], [17].

Laser bias current influences intermodulation through two mechanisms: the optical modulation index and the laser bandwidth. Implicit in the linear dependence of the intermodulation noise P_{im} on the digital modulation power P_{dig} (Fig. 5) is a quadratic dependence on the digital optical modulation index m_{dig}, where m_{dig} is defined as

$$m_{dig} = \frac{\sqrt{\frac{P_{dig}}{R}}}{I_B - I_{th}} = \frac{\Delta I}{I_B - I_{th}} \tag{4}$$

and R is 50 Ω. The intermodulation noise data given in Fig. 5 are replotted in Fig. 8 as a function of m_{dig} to explicitly demonstrate this dependence for three values of I_B. If the optical modulation index alone determines the intermodulation noise level, the three data curves in Fig. 8 should be collinear. The intermodulation noise for bias currents of $1.75I_{th}$ and $2I_{th}$ are approximately collinear; however, for $I_B = 2.75I_{th}$ the intermodulation noise is less for a given m_{dig} than for the lower bias currents. The lower intermodulation noise for the higher I_B is consistent with improved linearity of the laser diode resulting from an increased laser diode relaxation oscillation frequency. This is evident in Fig. 2, which shows the relaxation oscillation frequency is approximately 4 GHz for bias levels of $1.75I_{th}$ and $2I_{th}$, and is significantly higher for $I_B = 2.75I_{th}$. Therefore, increasing I_B lowers the intermodulation noise by decreasing m_{dig} and increasing the relaxation oscillation frequency.

4) Mixer Model: Extending the AM model developed in (2) and (3), the multiplexed microwave/baseband digital optical link can be viewed as a mixer (AM modulator) with the microwave signal as the local oscillator (LO) and the digital signal driving the intermediate frequency (IF) port.

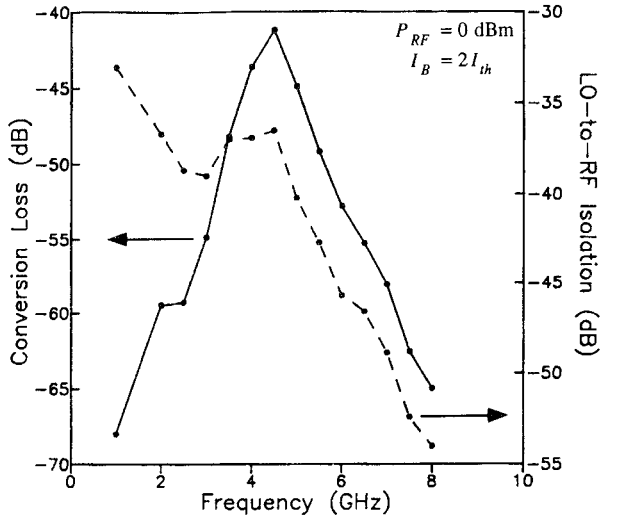

Fig. 9. Conversion loss and LO-to-RF isolation as a function of frequency where the FDM RF/baseband digital optical link is modeled as a mixer with up-conversion of the baseband digital signal by the "local oscillator" RF signal

In this case, the microwave optical link insertion loss represents the LO-to-RF isolation, and the conversion loss (L) is defined for the digital signal:

$$L = \frac{S_{\text{dig,out}}}{S_{\text{dig,in}}} \tag{5}$$

where $S_{\text{dig,in}}$ is the input digital signal power density (Fig. 3) and $S_{\text{dig,out}}$ is the output power density up-converted by the LO (parts (b) and (c) of Fig. 4). The behavior of these mixer parameters is illustrated in Fig. 9. The conversion loss has a maximum value of -41 dB at 4.5 GHz and decreases abruptly on either side. Fig. 9 can be used to estimate the intermodulation noise level for an arbitrary baseband waveform. Note, however, that these conversion loss values are for an RF power of $+0$ dBm and will vary proportionally to RF power as seen from (2).

B. Phase Noise

In microwave communication and radar systems, close-carrier phase noise is an important component of signal quality. Since LO signals typically have the most stringent phase noise requirement, and these signals are prime candidates for optical fiber signal distribution, it is critical that the effect of a baseband digital signal on microwave signal phase noise be quantified.

Measuring residual phase noise of the optical link independent of the RF source phase noise is the key factor in resolving possible phase noise degradation effects [17]. The residual phase noise of the optical link for $f_{\text{RF}} = 1.2$ GHz with no digital modulation is shown in Fig. 10(a). This illustrates the typical residual phase noise performance of microwave optical links: a $1/f$ decrease in the phase noise level between 1 Hz and 100 Hz offsets, reaching a flat noise floor determined by the laser relative intensity noise (RIN). Addition of digital modulation at 1 Mb/s (Fig. 10(b)) and 5 Mb/s (Fig. 10(c) does not affect the phase

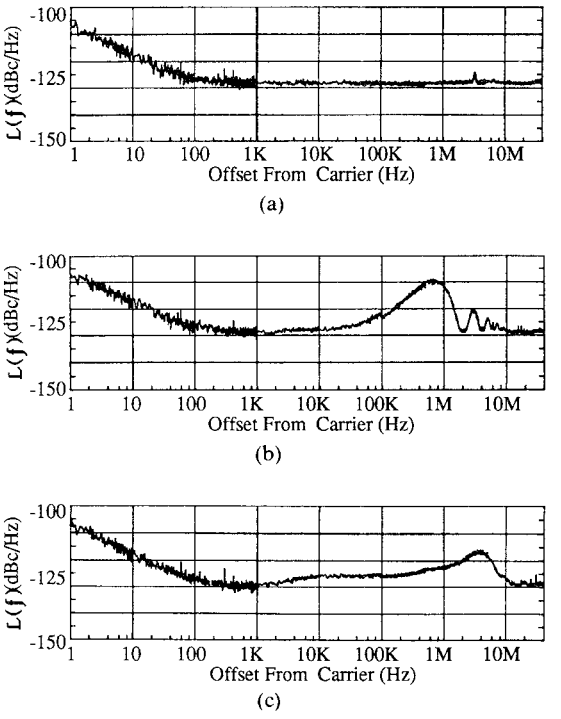

Fig. 10 Single-sideband residual phase noise of the FDM RF/baseband digital optical link for an RF signal at 1.2 GHz (a) with no digital modulation, (b) after addition of digital modulation at a 1 Mb/s data rate, and (c) after addition of digital modulation at a 5 Mb/s data rate.

noise at offset less than 1 kHz from the carrier. This demonstrates that, close to the carrier and independent of digital modulation, the optical link phase noise is lower than high-quality commercial signal sources such as an HP 8662A, which has a residual phase noise of approximately -122 dBc/Hz at a 1 kHz carrier offset.

At offsets greater than 1 kHz, the intermodulation noise becomes the dominant noise mechanism. Increasing the data rate lowers the peak intermodulation noise level, as observed in the previous section. Phase noise measurements, however, show that increasing the data rate also slightly increases the noise floor at offset frequencies in the 1 kHz to 100 kHz range, which could be important for certain system applications.

C. Digital Link Performance

Intermodulation distortion between the RF signal and the Manchester data in the baseband digital channel could degrade the digital link bit error rate (BER). The BER performance of the baseband digital link was characterized and plotted as a function of average received optical power P_{opt}. In this paper, P_{opt} does not include the optical power P_r emitted from the laser diode biased at I_B. The average received optical power P_{opt}, in context with the digital receiver, is interpreted as the digitally modulated optical power associated with the current ΔI. The digital receiver does not respond to changes in the laser diode bias current I_B, which was verified by observing no change in BER for a bias current range of 17.6 mA $< I_B <$ 40 mA for $\Delta I = 3$ mA and $I_{\text{th}} = 14.4$ mA.

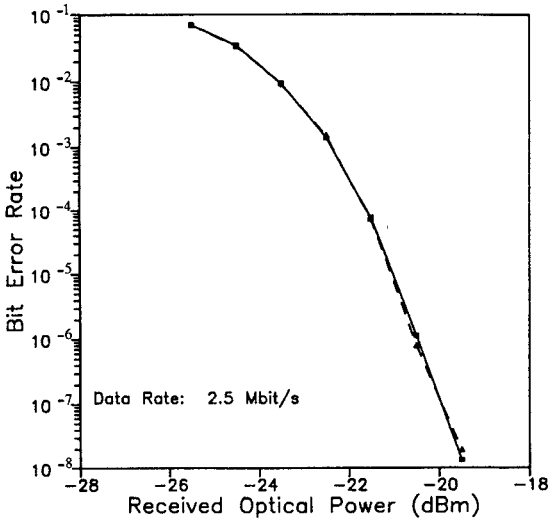

Fig. 11. Bit error rate as a function of average received optical power for the baseband digital data link. The solid curve is the nominal performance of the digital link without an RF signal present, while the dashed curve is data taken with a 4 GHz microwave signal present (+0 dBm input power).

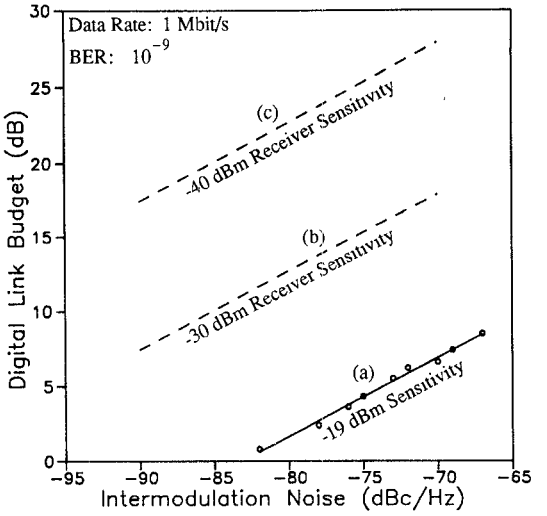

Fig. 12. Digital data link power budget as a function of the intermodulation noise power in the RF channel. The solid curve corresponds to measured data while the dashed curves are calculated for more sensitive digital receivers.

Fig. 11 presents the bit error rate as a function of average received optical power for the digital data link at a data rate of 2.5 Mb/s. There are two curves shown in the figure, where the solid curve corresponds to the baseline BER performance of the data link, and the dashed curve corresponds to the BER in the presence of a 4 GHz RF signal at a power level of +0 dBm. There was no significant degradation of BER performance due to harmonic distortion induced by intermodulation between the baseband and RF signals.

IV. RF and Digital System Performance Trade-off

Having shown that the RF channel second-order intermodulation noise P_{im} is proportional to the input baseband digital power P_{dig} and realizing that the digital link optical power budget also depends on P_{dig}, we can derive a direct relationship between the digital link power budget and P_{im}. Recalling from (4) that P_{dig} is proportional to ΔI^2 and that the digital optical power P_{opt} is proportional to ΔI, it follows that P_{im} is proportional to the square of P_{opt}. Since the digital link power budget is defined as the difference between P_{opt} and the receiver sensitivity, for a prescribed BER, it then follows that the digital power budget varies as the square root of P_{im}.

Curve (a) in Fig. 12 depicts the measured power budget for the baseband digital link as a function of the RF channel intermodulation noise power. Curves (b) and (c) represent calculated digital link power budgets for more sensitive receivers, which can be readily designed at this modest data rate [19]. Each curve has a slope of one half, demonstrating that lowering the intermodulation noise level by a given amount of power can be achieved by trading only the square root as much power from the digital link budget. Reducing the intermodulation noise from −70 to −80 dBc/Hz, for example, requires only a 5 dB reduction in the digital link budget.

V. Application Example

In phased arrays the digital information travels from a central source out to the array elements. Because the FDM RF/baseband optical link is unidirectional, the RF signal would be either a modulated transmission signal (transmit array) or the LO signal (receive array). This link would typically not be used for a received modulated signal, except perhaps to allow transmission of digital built-in-test information back to the central processor.

Typical spurious specifications for the transmit signals are < -30 dBc and < -60 dBc for LO signals. Assuming the phased array is to be used in a system having a 1 MHz signal bandwidth and that a +12 dB digital link budget is desired for using 1:16 optical divider networks in the array architecture, the required digital receiver sensitivity for a 1 Mb/s data rate can be determined from Fig. 12. To achieve the above spurious levels requires a maximum intermodulation noise of −90 dBc/Hz and −120 dBc/Hz for transmit and LO signals, respectively, corresponding to minimum receiver sensitivities of approximately −35 dBm and −50 dBm. These receiver sensitivities can be achieved using optoelectronic integrated circuit (OEIC) p-i-n/FET receivers [20]. Compatibility with OEIC technology is important for phased array antenna applications, enabling the optical signal distribution network to take advantage of the same cost, size, and reliability benefits derived from MMIC technology.

VI. Conclusion

We demonstrated and characterized a FDM multiplexed optical link that simultaneously transmits RF and baseband digital signals. This system represents a simple and inexpensive multiplexing approach for use in phased array signal distribution networks. Although the intermodulation noise generated in the RF channel can be prohibitive, we show that excellent RF phase noise performance is possible and that specific intermodulation noise levels can be

achieved at the expense of the baseband digital link budget. The applicability of this multiplexing approach for phased array antenna signal distribution will depend on the specific RF signal quality requirements and the performance of OEIC digital and analog receiver technology.

ACKNOWLEDGMENT

The authors are indebted to H. S. Babbitt and G. F. Providakes for many helpful discussions and to M. S. Booth, D. J. Martin, and A. B. Forbes for their laboratory work.

REFERENCES

[1] J. L. Guggenmous and R. L. Johnson, "Fiber based phased array antennas," *Proc. SPIE*, vol. 789, pp. 70–77, 1987.
[2] A. S. Daryoush, A. P. S. Khanna, K. Bhasin, and R. Kunnath, "Fiber optic links for millimeter wave communications satellites," in *IEEE MTT-S Int. Microwave Symp. Dig.*, May 1988, pp. 933–936.
[3] K. Bhasin and R. Kunnath, "Optically interconnected phased arrays," NASA Tech. Memorandum 100855, Mar. 1988.
[4] F. Semendy and E. Katzen, "Microwave fiberoptic links for phased arrays," *Proc. SPIE*, vol. 886, pp. 247–255, 1988.
[5] W. E. Stephens and T. R. Joseph, "System characteristics of direct modulated and externally modulated RF fiber-optic links," *J. Lightwave Technol.*, vol. LT-5, pp. 380–387, 1987.
[6] P. J. Heim, M. Hohman, and G. F. Providakes, "RF characterization of wideband optical link for interconnection of microwave RF subsystems for airborne communications satellite terminals," *Proc. SPIE*, vol. 840, pp. 143–145, 1987.
[7] H. Blauvelt and K. Lau, "High signal to noise operation of fiber optic links to 18 GHz," in *IEEE MTT-S Int. Microwave Symp. Dig.*, May 1988, pp. 979–980.
[8] H. Ishio, J. Minowa, and K. Nosu, "Review and status of wavelength-division multiplexing technology and its application," *J. Lightwave Technol.*, vol. LT-2, pp. 448–463, 1984.
[9] T. E. Darcie, "Subcarrier multiplexing for multiple-access lightwave networks," *J. Lightwave Technol.*, vol. LT-5, pp. 1103–1110, 1987.
[10] W. I. Way and C. Castelli, "Simultaneous transmission of 2 Gbit/s digital data and ten FM-TV analogue signals over 16.5 km SM fibre," *Electron. Lett.*, vol. 24, pp. 611–613, 1988.
[11] R. Olshansky, V. Lanzisera, and P. Hill, "Simultaneous transmission of 100 Mbit/s at baseband and 60 FM video channels for a wideband optical communication network," *Electron. Lett.*, vol. 24, pp. 1234–1235, 1988.
[12] C. N. Lo and L. S. Smoot, "Integrated fiber optic transmission of FM HDTV and 622 Mb/S data," in *IEEE MTT-S Int. Microwave Symp. Dig.*, June 1989, pp. 703–704.
[13] S. Haykin, *Communication Systems*. New York: Wiley, 1983, p. 119.
[14] K. Y. Lau and A. Yariv, "Intermodulation distortion in a directly modulated semiconductor injection laser," *Appl. Phys. Lett.*, vol. 45, no. 10, pp. 1034–1036, 1984.
[15] W. I. Way, "Large signal nonlinear distortion prediction for a single-mode laser diode under microwave modulation," *J. Lightwave Technol.*, vol. LT-5, pp. 305–315, 1987.
[16] T. E. Darcie, R. S. Tucker, and G. J. Sullivan, "Intermodulation and harmonic distortion in InGaAsP lasers," *Electron. Lett.*, vol. 21, pp. 665–666, 1985.
[17] W. I. Way, "Frequency dependent and frequency-independent nonlinear characteristics of a high-speed laser diode," in *IEEE MTT-S Int. Microwave Symp. Dig.*, May 1988, pp. 991–994.
[18] T. R. Faulkner and R. E. Temple, "Residual phase noise and AM noise measurements and techniques," Hewlett-Packard Part No. 03048-90011.
[19] G. Keiser, *Optical Fiber Communications*. New York: McGraw-Hill, 1983, p. 214.
[20] R. F. Leheny, "Optoelectronic integration: A technology for future telecommunication systems," *IEEE Circuits and Devices Magazine*, vol. 5, pp. 38–41, May 1989.

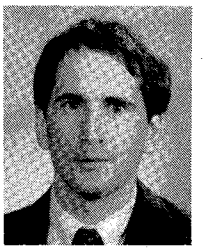

Peter J. Heim (M'89) received the A.B. and A.M. degrees in physics from Dartmouth College, Hanover, NH, in 1982 and 1984, respectively.

In 1984, he joined the MITRE Corporation as a Technical Staff member and is currently investigating optical signal distribution techniques for microwave and millimeter-wave phased array antennas. His other research interests include optoelectronic integrated circuits and MMIC optical interconnect technology.

Mr. Heim is a member of the American Physical Society and the Society of Photo-Optical Instrumentation Engineers.

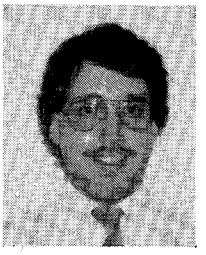

C. Phillip McClay (S'85–M'88) received the B.S. and M.S. degrees in electrical engineering from the University of Virginia, Charlottesville. He worked in the Semiconductor Device Laboratory from 1986 to 1988, where his graduate research focused on the fabrication of superconductive tunnel junctions for radio astronomy applications.

Since 1988 he has been employed as a Member of the Technical Staff at the MITRE Corporation, Bedford, MA. He is currently pursuing research in both optical signal distribution for phased array antenna applications and superconducting electronics for analog-to-digital conversion.